Optical Engineering

OpticalEngineering.SPIEDigitalLibrary.org

Processing grating structures on surfaces of wide-bandgap semiconductors using femtosecond laser and phase mask

Bo Gao
Tao Chen
Wei Cui
Cunxia Li
Jinhai Si
Xun Hou

SPIE.

Optical Engineering 54(12), 126106 (December 2015)

Processing grating structures on surfaces of wide-bandgap semiconductors using femtosecond laser and phase mask

Bo Gao,[a] Tao Chen,[a,*] Wei Cui,[a] Cunxia Li,[b] Jinhai Si,[a] and Xun Hou[a]
[a]Xi'an Jiaotong University, School of Electronics & Information Engineering, Key Laboratory for Physical Electronics and Devices of the Ministry of Education & Shaanxi Key Lab of Information Photonic Technique, Xianning West Road, Xi'an 710049, China
[b]Xi'an University of Technology, Department of Applied Physics, Yanxiang Road 58, Xi'an 710049, China

Abstract. Fabrication of grating structures on surfaces of wide-bandgap semiconductors, namely silicon carbide (SiC) and gallium nitride (GaN), was achieved using a femtosecond laser and a phase mask. The phase mask was used to produce stable interference patterns from the focused femtosecond laser to form the grating structures on the bulk materials. The effects of the irradiation power and time on the Bragg grating morphology that was formed on the SiC surface were studied. By optimizing the fabrication parameters, we successfully produced grating structures with uniform periods of 1.07 μm on SiC and GaN. The threshold powers necessary for grating structure formation on wide-bandgap semiconductors were investigated. It was found that the threshold powers for SiC and GaN were much smaller than those for silica glass. The reason for this difference is that the absorption of the incident laser light in SiC and GaN is a lower-order nonlinear absorption process compared to that in silica glass. *© 2015 Society of Photo-Optical Instrumentation Engineers (SPIE)* [DOI: 10.1117/1.OE.54.12.126106]

Keywords: femtosecond laser; laser interaction with matter; semiconductor materials.

Paper 151298 received Sep. 19, 2015; accepted for publication Nov. 9, 2015; published online Dec. 9, 2015.

1 Introduction

Wide-bandgap materials, such as silicon carbide (SiC) and gallium nitride (GaN), are of high technological importance as structures and substrates for microelectromechanical systems, light-emitting diodes, and laser diodes.[1–3] They possess the advantages of wide bandgaps, high breakdown electric fields, and high thermal conductivities. Grating structures are highly attractive because of their applicability in SiC optical temperature sensors and GaN distributed-feedback laser devices.[4,5] However, it is difficult to micromachine SiC and GaN due to their high hardnesses and high chemical stabilities.[6–8] Generally, the primary method of fabricating grating structures on wide-bandgap semiconductors is reactive-ion etching.[9,10] However, processing complexity is a significant drawback of this method.

Femtosecond lasers have become important tools for processing a variety of materials.[11–16] The advantages of using femtosecond laser pulses are that they radiate ultrahigh peak powers onto their targets and that they deliver energy into materials before thermal diffusion occurs, resulting in high precision and minimal thermal damage.[17] Many interesting nanostructures have been induced using femtosecond lasers; for example, synthesis of ultrafine Yb-doped Y_2O_3 nanoparticles,[18] which has great potential application to bioimaging due to its upconversion emission.[19] Femtosecond laser direct writing has been employed to micromachine grating structures on wide-bandgap materials.[4] However, it is difficult to fabricate grating structures with uniform periods of less than a few micrometers. Recently, inscribing a Bragg grating in an optical fiber using laser radiation and a phase mask has been proven to be a fast and effective technique.[20] Some research has been performed on the fabrication of volume gratings in bulk materials using femtosecond lasers and phase masks.[21] To the best of our knowledge, no reports have been published on the fabrication of Bragg gratings on the surfaces of SiC and GaN using this method.

In this paper, we introduce an efficient method for fabricating surface-grating structures using a femtosecond laser and a phase mask. A cylindrical-lens-focused 800-nm femtosecond laser beam was irradiated on the surfaces of the bulk materials through a phase mask. The phase mask was used to produce spatially modulated interference fields, which were capable of inducing grating structures on the bulk materials. The effects of the irradiation power and time on the Bragg grating morphology that was formed on the SiC surface were studied. By optimizing the fabrication parameters, we successfully produced grating structures with uniform periods of 1.07 μm on SiC, GaN, and silica glass. The threshold powers necessary to form the grating structures on these materials were investigated and compared.

2 Experimental Procedure

A schematic of grating structure fabrication with a femtosecond laser is shown in Fig. 1. The laser source was an amplified Ti:sapphire femtosecond laser system (Libra-USP-HE, Coherent Co.) with a pulse duration of 50 fs, central wavelength of 800 nm, and repetition rate of 1 kHz. The 12-mm-diameter Gaussian beam was focused by a cylindrical lens through a phase mask onto the bulk materials. The focal length of the cylindrical lens was 25 mm. The phase mask was made from a 2-mm-thick UV-grade fused silica slab. The period and groove line width of the phase mask

---

*Address all correspondence to: Tao Chen, E-mail: tchen@mail.xjtu.edu.cn

0091-3286/2015/$25.00 © 2015 SPIE

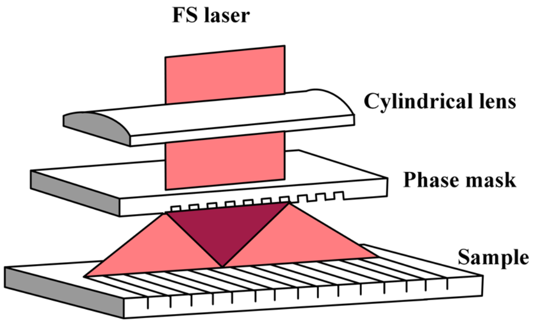

Fig. 1 Schematic of grating structure fabrication.

were 2.14 and 1.07 μm, respectively. The phase mask was a self-aligning interferometer that reliably produced a highly repeatable spatially modulated interference field. The first-order diffracted beams produced an interference pattern in a spatial overlap region behind the phase mask; this pattern was irradiated onto the sample surfaces to form the grating structures. The distance between the sample and phase mask was set to 3 mm. Thus, the diffracted beams of different order pairs $(0, \pm 1, \pm 2$, and so on) would not overlap spatially resulting from an order walk-off effect.[22] The diffraction efficiencies for the ±1-order diffracted beams were around 35%. The high-orders and zero-order diffraction were greatly suppressed. Hence, only ±1-order diffracted beams could induce grating structures on sample. The diffraction angles of the ±1-order diffracted beams were $\theta = \pm \arcsin(\lambda/\Lambda_{\text{pm}})$, where λ was the wavelength of the incident light and Λ_{pm} was the phase mask period. The periods of interference pattern of ±1-order diffracted beams and their resulted grating structures on the sample were $\Lambda_g = \lambda/2 \sin\theta$. Thus, we could obtain $\Lambda_g = \Lambda_{\text{pm}}/2$. This means that the period of the formed grating structures was half of the phase mask period. In our experiments, grating structures with a period of 1.07 μm were obtained on the surface of bulk materials.

Bulk 6H-SiC, GaN, and silica glass were used in our experiments. The thicknesses of the 6H-SiC, GaN, and silica glass were 350, 300, and 1000 μm, respectively. For each material, the sample was cleaned using an ultrasonic machine with acetone and then with deionized water for 10 min each. Subsequently, the sample was mounted on the translation stage, and the femtosecond laser beam was focused on the sample through the cylindrical lens. The sample was placed on the focal plane of the cylindrical lens. According to the free-space Gaussian beam optics, the width of the focal spot size was $W = 2\lambda f/\pi\omega_0 = 2.1$ μm, where f was the focal length of the cylindrical lens and ω_0 was the incident beam waist. Then the sample was exposed to write the gratings. The resulted grating structures were directly observable under a standard optical microscope.

3 Results and Discussion

Figures 2(a)–2(e) show the grating structures on the surface of SiC as observed under a microscope with 100× magnification. The femtosecond laser powers were set to 150, 200, 250, 300, and 350 mW, and the exposure time was set to 0.1 s. In Fig. 2(a), the grating structure on the SiC surface is observable. However, the grating grooves are absent in some areas. This absence may have occurred because for a power of 150 mW, the light intensity was only slightly greater than the threshold necessary for grating formation and because the formation of grating grooves is very sensitive to spatial fluctuations in the light intensity. As the laser power increases to more than 200 mW, the laser fluence reaches the ablation threshold in the most-irradiated zone, resulting in regularity of the grating structure. For a laser power of 250 mW, the grating structures are highly uniform, as shown in Fig. 2(c), and have periods of about 1.07 μm, which is half of the phase mask period. When the laser power was set to 300 and 350 mW, as shown in Figs. 2(d) and 2(e), laser-induced trenches were formed in the center of the grating zone, and the grating structures were damaged due to the high-energy laser irradiation. In order to investigate the dependence of the structure morphology on the exposure time, we also performed experiments using different exposure times, specifically 0.02, 0.05, 0.1, and 0.2 s. When the laser power and exposure time were set to 250 mW and 0.1 s, respectively, highly uniform grating structures could be obtained on the SiC surface very efficiently and quickly. The average groove depth of the grating was estimated to be about 300 nm from confocal microscopy measurement results. The total length and width of the formed grating structures were around 8 mm and 7 μm, respectively. By scanning the sample surface along the grating groove direction, we could obtain large-area gratings. Then diffraction effects of samples were characterized by using a 633-nm He-Ne laser. The diffraction pattern was irradiated on a paper screen, then photographed. For the sample shown in Fig. 2(c), its diffraction pattern is shown in Fig. 2(f). We can see that the diffraction pattern is clear to distinguish at 0 and ±1 orders. The higher order diffractions were absent.

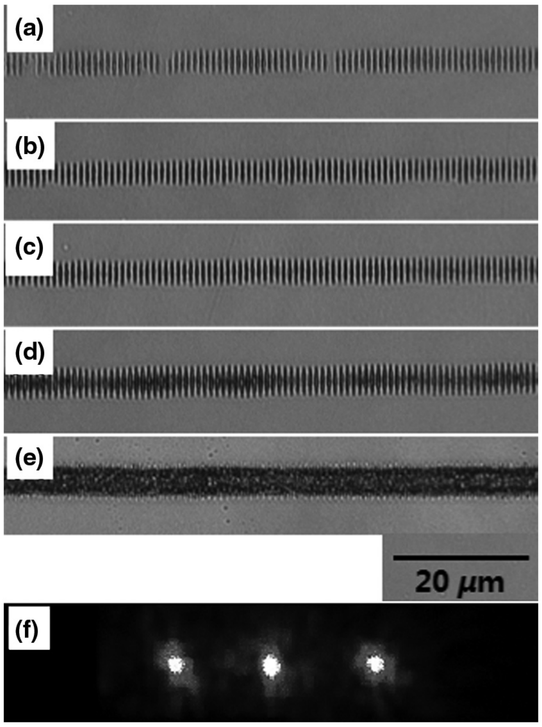

Fig. 2 Grating structures on SiC surface formed under laser powers of (a) 150 mW, (b) 200 mW, (c) 250 mW, (d) 300 mW, and (e) 350 mW. (f) Diffraction pattern of SiC sample fabricated under 250-mW laser power by a camera.

Furthermore, we studied the fabrication of Bragg grating structures on GaN and silica glass. The threshold laser powers necessary to produce grating structures on the surfaces of the wide-bandgap semiconductors (SiC and GaN) and silica glass using a femtosecond laser and a phase mask were investigated and compared. The experimental conditions and setups were the same as those described earlier. To determine the threshold, we decreased the laser power until no structural change occurred on the SiC surface. In our experiments, the threshold laser powers necessary to fabricate structures on the surfaces of SiC, GaN, and silica glass were around 100, 120, and 750 mW, respectively. In order to form regular grating structures, the laser power was optimized for each sample. Figure 3 shows the grating structures on the surfaces of SiC, GaN, and silica glass as observed under a microscope with 50× magnification. The employed femtosecond laser powers were 220, 250, and 800 mW for the SiC, GaN, and silica glass, respectively, and the exposure time was set to 0.1 s. As shown in Fig. 3, the grating structures have excellent uniformity and periods of 1.07 μm.

According to the above results, the threshold and optimal powers for SiC and GaN were much smaller than those for silica glass. The transmittances of SiC, GaN, and silica glass were characterized to clarify the reason for this difference. Figure 4 shows the transmittance spectra of SiC, GaN, and silica glass, in which the reflections from the samples have been considered and subtracted. We can see that there is almost no absorption for silica glass, whereas SiC shows the strongest absorption among the three samples for a wavelength of 800 nm, reaching about 50%. In addition, SiC shows the strongest absorption at about 625 nm. This high absorption is evident because the SiC used in our experiment contained impurities. The transmittances of SiC and GaN become zero at wavelengths shorter than 390 and 375 nm, respectively. The photon energies at these two wavelengths just correspond to the bandgaps of these materials. Hence, the effective nonlinear absorption at 800 nm for the two wide-bandgap semiconductors occurred through an absorption process involving at least three photons. In addition, the 800-nm laser reaction with silica glass mainly arose from more than four-photon absorption, because no strong absorption is evident until the wavelength becomes shorter than about 200 nm. Therefore, the threshold and optimal powers for the wide-bandgap semiconductors were much smaller than those for silica glass. In addition, although SiC shows a linear absorption at 800 nm that is stronger than that of GaN, the difference between their threshold powers was very small, implying that the nonlinear effect was dominant in the interactions between the 800-nm femtosecond laser and each of the semiconductor materials. In the process of laser micromachining, the nonlinear processes that cause breakdown are avalanche ionization and multiphoton ionization.[23] For moderate laser fluences, avalanche ionization is dominant, whereas multiphoton ionization requires more intense light. Generally, seed electrons required for avalanche ionization could originate from metallic impurities or the thermal or linear optical ionization of the shallow energy levels of inclusions in transparent materials. Although the linear absorption due to the impurities in SiC may facilitate the generation of seeded electrons for avalanche ionization, the nonlinear process was dominant in the formation of the grating structures on SiC and GaN. Therefore, the threshold powers for SiC and GaN were almost the same.

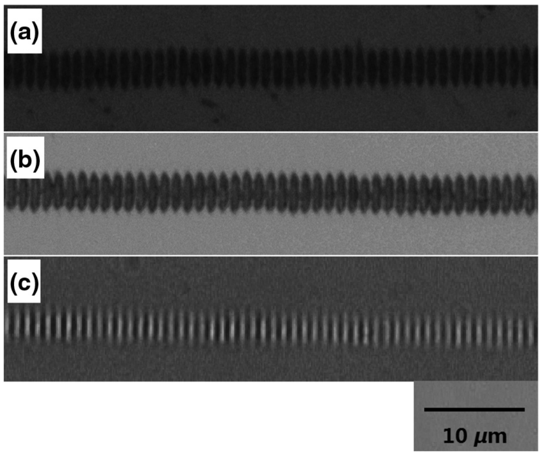

Fig. 3 Grating structures on surfaces of (a) SiC, (b) GaN, and (c) silica glass.

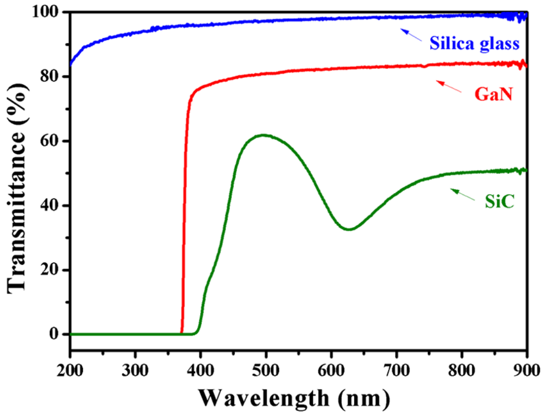

Fig. 4 Transmittance spectra of SiC, GaN, and silica glass.

4 Conclusion

In conclusion, we introduced an efficient method of fabricating surface-grating structures on wide-bandgap semiconductors using a femtosecond laser and a phase mask. A cylindrical-lens-focused 800-nm femtosecond laser beam was irradiated on the surfaces of bulk materials through a phase mask. The phase mask was used to produce an interference pattern in a spatial overlap region to form the grating structures. We successfully fabricated grating structures with uniform 1.07 μm periods on SiC, GaN, and silica glass. We found that the threshold powers for the wide-bandgap semiconductors were much smaller than those for silica glass. The reason for this difference is that the absorption of the incident laser in SiC and GaN occurs through a nonlinear absorption process lower in order than that in silica glass. This method was proven to be a more effective and versatile approach to grating fabrication.

Acknowledgments

This work was supported by the Collaborative Innovation Center of Suzhou Nano Science and Technology. The authors gratefully acknowledge the financial support for this work provided by the National Basic Research Program of China (973 Program) under Grant No. 2012CB921804, by the National Natural Science Foundation of China (NSFC) under Grant Nos. 11204236 and 61308006, and by the China Postdoctoral Science Foundation funded project under Grant No. 2013M542351.

References

1. M. Mehregany and C. A. Zorman, "SiC MEMS: opportunities and challenges for applications in harsh environments," *Thin Solid Films* **355**(99), 518–524 (1999).
2. S. Nakamura et al., "High-brightness InGaN blue, green, and yellow light-emitting diodes with quantum well structures," *Jpn. J. Appl. Phys.* **34**(7A), L797–L799 (1995).
3. S. Nakamura et al., "InGaN-based multi-quantum-well-structure laser diodes," *Jpn. J. Appl. Phys.* **35**(2B), L74–L76 (1996).
4. G. L. DesAutels et al., "Optical temperature sensor and thermal expansion measurement using a femtosecond micromachined grating in 6H-SiC," *Appl. Opt.* **47**(21), 3773–3777 (2008).
5. R. Werner et al., "High-resolution patterning and characterization of optically pumped first-order GaN DFB lasers," *Physica E* **7**(3), 915–918 (2000).
6. G. F. Mclane and J. R. Flemish, "High etch rates of SiC in magnetron enhanced SF_6 plasmas," *Appl. Phys. Lett.* **68**(26), 3755–3757 (1996).
7. M. R. Melloch, J. A. Cooper, Jr., and D. J. Larkin, "Fundamentals of SiC-based device processing," *MRS Bull.* **22**(3), 42–49 (1997).
8. J. C. Zolper and R. J. Shul, "Implantation and dry etching of group III-nitride semiconductors," *MRS Bull.* **22**(2), 36–43 (1997).
9. Y. J. Wang, F. R. Hu, and K. Hane, "Patterned growth of InGaN/GaN quantum wells on freestanding GaN grating by molecular beam epitaxy," *Nanoscale Res. Lett.* **6**, 117 (2011).
10. J. H. Lee et al., "Polarization-dependent GaN surface grating reflector for short wavelength applications," *Opt. Express* **17**(25), 22535–22542 (2009).
11. S. Backus et al., "High power ultrafast lasers," *Rev. Sci. Instrum.* **69**(3), 1207–1223 (1998).
12. U. Keller, "Recent developments in compact ultrafast lasers," *Nature* **424**(6950), 831–838 (2003).
13. J. R. Qiu, "Femtosecond laser-induced microstructures in glasses and applications in micro-optics," *Chem. Rec.* **4**(1), 50–58 (2004).
14. K. Miura et al., "Formation of Si structure in glass with a femtosecond laser," *Appl. Phys. A* **93**(1), 183–188 (2008).
15. N. Zhang et al., "Fabrication of long-period fibre gratings using 800 nm femtosecond laser pulses," *Chin. Phys. Lett.* **23**(12), 3281 (2006).
16. F. He et al., "Rapid fabrication of optical volume gratings in Foturan glass by femtosecond laser micromachining," *Appl. Phys. A* **97**(4), 853–857 (2009).
17. G. Rice et al., "Micromachining of gallium nitride, sapphire, and silicon carbide with ultrashort pulses," *Proc. SPIE* **5147**, 299 (2003).
18. C. B. Zheng et al., "Femtosecond pulsed laser induced synthesis of ultrafine Y_2O_3: Pr, Yb nanoparticles with improved upconversion efficiency," *Chem. Phys. Lett.* **496**(4), 316–320 (2010).
19. D. Y. Li et al., "Effect of Li^+ ions on enhancement of near-infrared upconversion emission in $Y_2O_3:Tm^{3+}/Yb^{3+}$ nanocrystals," *J. Appl. Phys.* **112**(9), 094701 (2012).
20. G. C. B. Lee et al., "Femtosecond laser inscribed phase masks for fibre Bragg grating sensor inscription," *Proc. SPIE* **8421**, 84214V (2012).
21. C. Voigtländer et al., "Inscription of high contrast volume Bragg gratings in fused silica with femtosecond laser pulses," *Appl. Phys. A Mater.* **102**(1), 35–38 (2011).
22. C. W. Smelser, D. Grobnic, and S. J. Mihailov, "Generation of pure two-beam interference grating structures in an optical fiber with a femtosecond infrared source and a phase mask," *Opt. Lett.* **29**(15), 1730–1732 (2004).
23. X. Liu, D. Du, and G Mourou, "Laser ablation and micromachining with ultrashort laser pulses," *IEEE J. Quantum Electron.* **33**(10), 1706–1716 (1997).

Bo Gao received his BS degree in electronic science and technology from Xi'an University of Technology, Xi'an, China, in 2007 and his MS degree in medical physics from Heidelberg University, Germany, in 2010. He is currently working toward his PhD at Xi'an Jiaotong University, Xi'an, China. His research interests include optoelectronic devices and femtosecond laser fabrication.

Tao Chen received his PhD in electronic science and technology from Xi'an Jiaotong University in 2011. Currently, he is a lecturer in Xi'an Jiaotong University. His current interests include ultrafast nonlinear optics and femtosecond micromachining.

Biographies for the other authors are not available.